Metformin suppresses foam cell formation, inflammation and ferroptosis via the AMPK/ERK signaling pathway in ox-LDL-induced THP-1 monocytes

YIHAN ZHAO[1,2], YIZHEN ZHAO[3], YUAN TIAN[4] and YANG ZHOU[5]

[1]Department of Cardiology, Sichuan Academy of Medical Sciences and Sichuan Provincial People's Hospital, School of Medicine, University of Electronic Science and Technology of China, Chengdu, Sichuan 610072; [2]The Key Laboratory of Cardiovascular Disease of Wenzhou, Department of Cardiology, The First Affiliated Hospital of Wenzhou Medical University, Wenzhou, Zhejiang 325000; [3]Department of Neurosurgery, North Sichuan Medical College, Nanchong, Sichuan 637000; [4]Clinical Research Center, The Affiliated Hospital of Guizhou Medical University, Guiyang, Guizhou 550000; [5]Department of Vascular Surgery, Deyang People's Hospital, Deyang, Sichuan 618000, P.R. China

Received April 20, 2022; Accepted August 3, 2022

DOI: 10.3892/etm.2022.11573

Abstract. Numerous studies have shown that the formation of foam cells is of vital importance in the process of atherosclerosis. The aim of the present study was to assess the effects of metformin on foam cell formation in oxidized low-density lipoprotein (ox-LDL)-treated THP-1 cells and explore its associated mechanism of action. Human monocytic THP-1 cells were pretreated with metformin for 2 h and subsequently treated with ox-LDL for 24 h. The data indicated that metformin significantly inhibited lipid accumulation in ox-LDL-treated THP-1 cells by decreasing the expression of scavenger receptor A, cluster of differentiation 36 and adipocyte enhancer-binding protein 1. In addition, metformin increased the expression levels of scavenger receptor B1 and ATP binding cassette transporter G1 and suppresses the esterification of free cholesterol. Furthermore, it markedly inhibited ferroptosis (reflected by the upregulation of glutathione peroxidase glutathione peroxidase 4 and the downregulation of Heme oxygenase-1). In addition, it caused a marked suppression in the expression levels of cysteinyl aspartate specific proteinase-1, IL-1β, NOD-like receptor protein 3, IL-18 secretion and in the levels of oxidative stress. Metformin attenuated the activation of ERK and facilitated the phosphorylation of 5' adenosine monophosphate-activated protein kinase (AMPK). Treatment of THP-1 cells with an ERK inhibitor reversed these effects, while inhibition of AMPK activity exacerbated the effects noted in ox-LDL-treated THP-1 cells. In conclusion, the present study suggested that metformin suppressed foam cell formation, inflammatory responses and inhibited ferroptosis in ox-LDL-treated macrophages via the AMPK/ERK signaling pathway.

Correspondence to: Dr Yuan Tian, Clinical Research Center, The Affiliated Hospital of Guizhou Medical University, 28 Guiyi Street, Guiyang, Guizhou 550000, P.R. China
E-mail: tianyuan@stu.gmc.edu.cn

Dr Yang Zhou, Department of Vascular Surgery, Deyang People's Hospital, 173 Section 1, Taishan North Road, Deyang, Sichuan 618000, P.R. China
E-mail: 185610561@qq.com

Key words: atherosclerosis, metformin, oxidized low-density lipoprotein, foam cells, ferroptosis, inflammation

Introduction

Atherosclerosis is a chronic disease and a major contributing factor to high morbidity and mortality worldwide (1). Foam cells are essential components of atherosclerosis (2). In the process of arteriosclerosis, monocytes adhere to endothelial cells, invade the subendothelial layer and differentiate into macrophages. The macrophages, in turn, engulf lipids, secrete proinflammatory cytokines and promote foam cell formation (3). This leads to lipid overload, inflammation and oxidative stress in oxidized LDL (ox-LDL)-treated macrophages (4-6). All these factors result in plaque formation, rupture, bleeding and blockage of the vascular cavity, which promote the development of serious cardiovascular events (7). Therefore, it is beneficial to decrease the levels of lipids in macrophages to suppress the process of atherosclerosis.

Ferroptosis is a recently defined form of programmed cell death that is induced by iron-dependent lipid peroxidation and differs from apoptosis, cell necrosis and autophagy (8). It is characterized by iron deposition, lipid peroxidation and decreased expression of glutathione peroxidase 4 (Gpx4) in cells (9,10). The induction of oxidative stress and lipid peroxidation caused by ferroptosis indicates a possible correlation between ferroptosis and atherosclerosis. Recently, a number of studies have demonstrated that ferroptosis is involved in the pathophysiological process of atherosclerosis (11,12). A previous study suggests that iron overload and incubation with ox-LDL and lipopolysaccharide/IFN-γ increase the number of

M1 proinflammatory-phenotype macrophages produced and the inflammatory response (13), resulting in the induction of ferroptosis in atheroma (14).

Metformin is a therapeutic drug used for type 2 diabetes (15). Studies have shown that metformin can reduce the risk of breast cancer (16), cervical cancer (17,18), prostate cancer (19), gastric cancer (20) and other types of cancer. Metformin promotes an anti-inflammatory effect on macrophages by suppressing fatty acid synthase-dependent palmitoylation of AKT (21). Clinical trials have also demonstrated the protective role of metformin against abdominal aortic aneurysms (22). Studies have suggested that metformin can alleviate angiotensin-induced cardiomyocyte hypertrophy (23) and prevent excessive myocardial fibrosis and ventricular remodeling following myocardial infarction (24). Furthermore, metformin mitigates the progression of atherosclerosis by suppressing monocyte-to-macrophage differentiation, induction of inflammatory responses and smooth muscle cell migration (25-27).

However, the specific mechanism by which metformin affects the formation of foam cells remains to be elucidated. Therefore, the purpose of the present study was to determine whether metformin acts as a protective factor in the formation of foam cells and to identify its potential mechanism of action.

Materials and methods

Cell culture. The human monocytic cell line (THP-1 cells; American Type Culture Collection) was cultured in RPMI 1640 medium (HyClone; Cytiva), supplemented with 10% FBS (Gibco; Thermo Fisher Scientific, Inc.) and 1% penicillin/streptomycin solution, at 37˚C in the presence of 5% CO_2. To induce macrophage differentiation, THP-1 cells were incubated with 100 nM phorbol 12-myristate 13-acetate (PMA; MilliporeSigma) for 48 h in 6-well plates at a density of $5x10^5$ cells/ml (28). Subsequently, the cells were pretreated for 2 h prior to incubation with ox-LDL (Guangzhou Yiyuan Biological Technology Co. Ltd.) for 24 h with one of the following compounds each time: Metformin, PD98059 (a MAPK/ERK inhibitor), compound C [5' adenosine monophosphate-activated protein kinase (AMPK) inhibitor], erastin (a ferroptosis agonist), or ferrostatin-1 (a ferroptosis inhibitor).

Cytotoxicity test with metformin. THP-1 cells were seeded in 96-well plates at a density of $1x10^5$ cells/well and incubated with different concentrations (5, 10, 25, 50 and 100 μM) of metformin. To explore the time point of metformin pretreatment in an ox-LDL stimulated macrophage model, THP-1 cells were also incubated at different time points (0, 2, 4, 6, 8, 12 and 24 h) of metformin. Cell Counting kit-8 (CCK-8) assay (Nanjing Jiancheng Bioengineering Institute) was used to measure the cytotoxicity of metformin (Beijing Jialin Pharmaceutical Co., Ltd.).

Western blot analysis. After incubation with oxLDL for 24 h, the supernatant was removed and the total protein extraction reagent (Boster Biological Technology) added. The protein was determined by using a BCA Protein Concentration Assay kit (Beijing Solarbio Science & Technology Co., Ltd.). A total of 20 μg protein was separated by 10 or 12% SDS-PAGE gels and subsequently blotted onto a nitrocellulose membrane. The membrane was blocked with 5% bovine serum albumin (BSA; Beijing Solarbio Science & Technology Co., Ltd.) at room temperature for 2 h, and subsequently incubated with primary antibodies overnight. These included anti-Gpx4 (cat. no. ER1803-15; 1:1,000), anti-scavenger receptor A (SRA; cat. no. ER1913-21; 1:1,000), anti-adipocyte enhancer-binding protein 1 (AEBP1; cat. no. ER61507; 1:1,000), anti-IL-1β (cat. no. ET1701-39; 1:1,000) and anti-GAPDH (cat. no. ER1706-83; 1:1,000; all from Huabio); anti-heme oxygenase-1 (Hmox-1; cat. no. ab269503; 1:1,000), anti-scavenger receptor class B type 1 (SR-B1; cat. no. ab217318; 1:1,000) and anti-ATP binding cassette transporter G1 (and ABCG1; cat. no. EP1366Y; 1:1,000; all from Abcam); anti-cluster of differentiation (CD) 36 (cat. no. 14347; 1:1,000), anti-caspase 1 (cat. no. 24232; 1:1,000), anti-phos-ERK (cat. no. 4695S; 1:1,000), anti-ERK (cat. no. 4370S; 1:1,000) and anti-NOD-like receptor protein 3 (NLRP3; cat. no. 13158; 1:1,000; all from Cell Signaling Technology, Inc.) and anti-AMPK (cat. no. AF6423; 1:1,000, Affinity), anti-phosphorylated (p) AMPK (cat. no. AF3423; 1:1,000; both from Affinity Biosciences, Ltd.) in 1% BSA overnight at 4˚C. The membranes were washed and incubated with horseradish peroxidase-conjugated secondary antibodies (cat. no. NB101H; 1:2,000; Huabio). Proteins were visualized by the Tinon ECL chemiluminescent reagent (Tanon Science and Technology Co., Ltd.). The results were analyzed using the Tanon 5200 and ImageJ 1.52a software (National Institutes of Health).

Oil Red O staining. Ox-LDL was purchased from Guangzhou Yiyuan Biotechnology Co., Ltd. Following incubation with ox-LDL at 37˚C for 24 h, the cells were washed with PBS thrice and fixed with 4% paraformaldehyde at room temperature for 20 min. The cells were stained with 60% Oil Red O solution and incubated for 20 min at room temperature according to the manufacturer's instructions. The excess dye solution was subsequently removed by washing with 60% isopropanol alcohol. Images were captured of the stained cells by a fluorescent microscope (magnification, x400; Olympus Corporation). A total of four fields of view were randomly observed in each group.

Dil-labeled-ox-LDL (dil-ox-LDL) uptake assay. Dil-ox-LDL was purchased from Guangzhou Yiyuan Biotechnology Co., Ltd. THP-1 cells were incubated with dil-ox-LDL (50 μg/ml) at 37˚C for 24 h. Subsequently, the cells were washed with PBS thrice prior to mounting with 4',6-diamidino-2-phenylindole in the dark for 5 min. Images were captured of the stained cells by a fluorescent microscope (magnification, x400; Olympus Corporation). A total of four fields of view were randomly observed in each group.

Cholesterol content analysis. Following incubation with ox-LDL at 37˚C for 48 h, the cells were collected for the measurement of cholesterol content using a commercial tissue cell free cholesterol enzymatic assay kit and a tissue cell total cholesterol enzymatic assay kit Applygen Technologies, Inc. A microplate reader was also used to record the absorbance readings. Finally, the free cholesterol content was subtracted from the total cholesterol content to determine the cholesterol ester content and the cholesterol ester/total cholesterol ratio was estimated.

Detection of superoxide dismutase (SOD) activity and malondialdehyde (MDA) levels. THP-1 cells were treated as previously described. The cells were washed thrice with PBS and the activity levels of SOD and the concentration levels of MDA in the cells were measured using the corresponding kits (Beyotime Institute of Biotechnology).

Cytokine measurements. The expression levels of IL-1β and IL-18 in ox-LDL-treated THP-1 cells were detected by specific ELISA kits (BP-E10081 and BP-E10092; Shanghai Boyun Bio). The final concentration levels were calculated from the absorbance values of each of the samples based on the plot obtained from the standard curve.

Statistical analysis. The data are presented as mean ± standard error of the mean. The statistical significance of the differences between the groups was determined using GraphPad Pro Prism 6.0 (GraphPad Software, Inc.). The comparison of multiple groups was performed using one-way analysis of variance followed by Tukey's test. $P<0.05$ was considered to indicate a statistically significant difference.

Results

Metformin hinders the formation of foam cells in ox-LDL-treated THP-1 cells. Initially, the cytotoxicity of metformin was assessed against THP-1 cells using the CCK-8 assay. As shown in Fig. 1A, incubation of the cells with 25 μM metformin for 24 h caused no effect on cell viability, whereas THP-1 cells treated with 50 and 100 μM metformin exhibited a significant reduction in cell viability. Consequently, the concentration of 25 μM was selected for further analyses. As shown in Fig. 1B, there was no decrease in cell viability as time was prolonged, so 2 h was selected for further analyses. THP-1 cells were seeded in 6-well plates at a concentration of $1x10^5$ cells/well and subsequently incubated in the presence of 100 nM PMA. The cells were then exposed to 50 nM ox-LDL for 24 h and the lipid content in THP-1 cells was detected by Oil Red O staining. The images were observed using light microscopy. THP-1 cells exposed to ox-LDL indicated higher lipid accumulation compared with that of the control PMA group; conversely, THP-1 cells pretreated with metformin prior to exposure to ox-LDL exhibited lower lipid content compared with the ox-LDL group (Fig. 1C). The measurement of the dil-oxLDL confirmed these results (Fig. 1E), indicating that metformin suppressed the formation of foam cells in ox-LDL-treated THP-1 cells.

Metformin reduces cholesterol content in foam cells. To measure the cholesterol content in foam cells, THP-1 cells were seeded in 6-well plates at a concentration of $5x10^5$ cells/well. THP-1 cells pretreated with metformin indicated lower contents of cholesterol ester and total cholesterol content and higher content of free cholesterol compared with the corresponding cholesterol contents noted in the ox-LDL group (Fig. 1D); consequently, it was inferred that metformin suppressed the esterification of free cholesterol in ox-LDL-treated foam cells and decreased total cholesterol levels in macrophages.

Metformin increases cholesterol efflux and decreases cholesterol influx in foam cells. THP-1 cells were pretreated with metformin for 2 h prior to their exposure to ox-LDL for 24 h and the expression levels of SRA, CD36, AEBP1, SR-B1 and ABCG1 were examined by western blotting. The results indicated that metformin increased the expression levels of SR-B1 and ABCG1 (Fig. 2E and F), while decreasing the expression levels of SRA, CD36 and AEBP1 (Fig. 2B-D). This indicated that metformin inhibited foam cell formation by increasing and decreasing cholesterol efflux in ox-LDL-treated foam cells.

Metformin decreases inflammation levels in ox-LDL-treated macrophages. To measure the inflammation levels of foam cells, the expression levels of caspase-1, IL-1β and NLRP3 were examined by western blotting; additionally, IL-1β and IL-18 levels in 48-h culture supernatants were measured by ELISA. The data indicated that a 2-h pretreatment period of the cells with metformin resulted in a reduction of the ox-LDL-mediated increase in caspase-1, IL-1β, NLRP3 (Fig. 3B-D), IL-1β and IL-18 levels (Fig. 3E and F), illustrating that metformin could attenuate the levels of inflammation in ox-LDL-treated foam cells.

Metformin inhibits ferroptosis in ox-LDL-treated macrophages. The cells were treated as previously described and the expression levels of Gpx4 and Hmox-1 were examined by western blotting. The concentration levels of MDA and the activity levels of SOD were detected using the lipid oxidation detection kit and the total SOD activity detection kit, respectively. The results indicated that the expression levels of Gpx4 and SOD were higher in metformin-pretreated macrophages compared with those noted in the ox-LDL group, while the expression levels of Hmox-1 and MDA were lower compared with those of the ox-LDL group (Fig. 4A-C). Moreover, when the cells were co-incubated with erastin or ferrostatin-1 and ox-LDL, metformin treatment Partially improved cell viability and indicated lower ferroptosis levels (reflected by the decreased levels of Hmox-1 and MDA and the increased expression levels of Gpx4 and SOD (Fig. 4D-G). These findings indicated that metformin could alleviate ferroptosis in foam cells.

Metformin decreases the activation of ERK and increases the phosphorylation of the AMPK signaling pathway. THP-1 cells were pretreated with metformin for 2 h prior to exposure to ox-LDL for 24 h and the expression levels of AMPK, pAMPK, ERK and pERK were detected. Metformin decreased the activation of the ERK signaling pathway and increased the phosphorylation of the AMPK signaling pathway (Fig. 5A and B). Subsequently, the direct effects of both the AMPK and ERK signaling pathways were investigated. In ox-LDL-treated THP-1 cells, the AMPK inhibitor increased lipid accumulation (Fig. 5C) by decreasing the downregulation of ABCG1 and SR-B1 expression levels and by increasing the upregulation of SRA1, CD36 and AEBP1 expression levels (Fig. 6A and B). Concomitantly, it improved the expression levels of inflammatory indicators (caspase-1, IL-1β, NLRP3; Fig. 6C and D) as well as the levels of ferroptosis (reflected by the decreased levels of Gpx4 and SOD and the increased levels of Hmox-1 and MDA; Fig. 6E-G). In contrast to these findings, administration of an ERK inhibitor produced the opposite results (Fig. 6A-G).

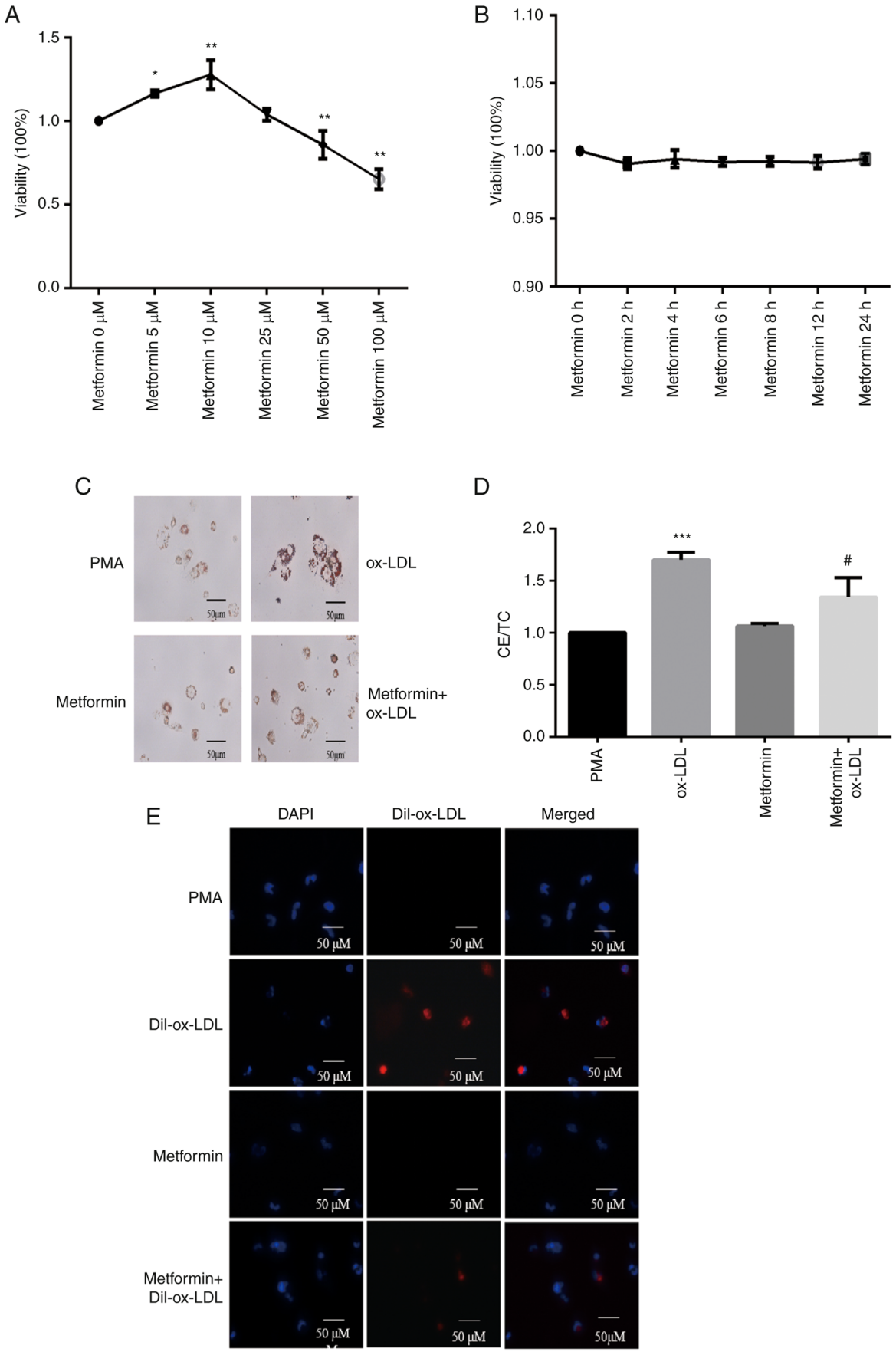

Figure 1. Effects of metformin on the formation of foam cells. (A and B) Cell viability was assessed by the CCK-8 assay. (C) The formation of foam cells was detected by Oil Red O staining. (D) The levels of cholesterol ester/total cholesterol in ox-LDL-treated macrophages were detected by a commercial tissue cell free cholesterol enzymatic assay kit and a tissue cell total cholesterol enzymatic determination kit. (E) Cholesterol uptake, detected by the dil-ox-LDL assay. Scale bar=50 μM. *P<0.05 vs. the control group, **P<0.01 vs. the control group, ***P<0.001 vs. the PMA group, $^{\#}$P<0.05 vs. the ox-LDL group. CCK-8, Cell Counting Kit-8; ox-LDL, oxidized low-density lipoprotein; dil-ox-LDL, dil-labeled-ox-LDL; PMA, phorbol 12-myristate 13-acetate.

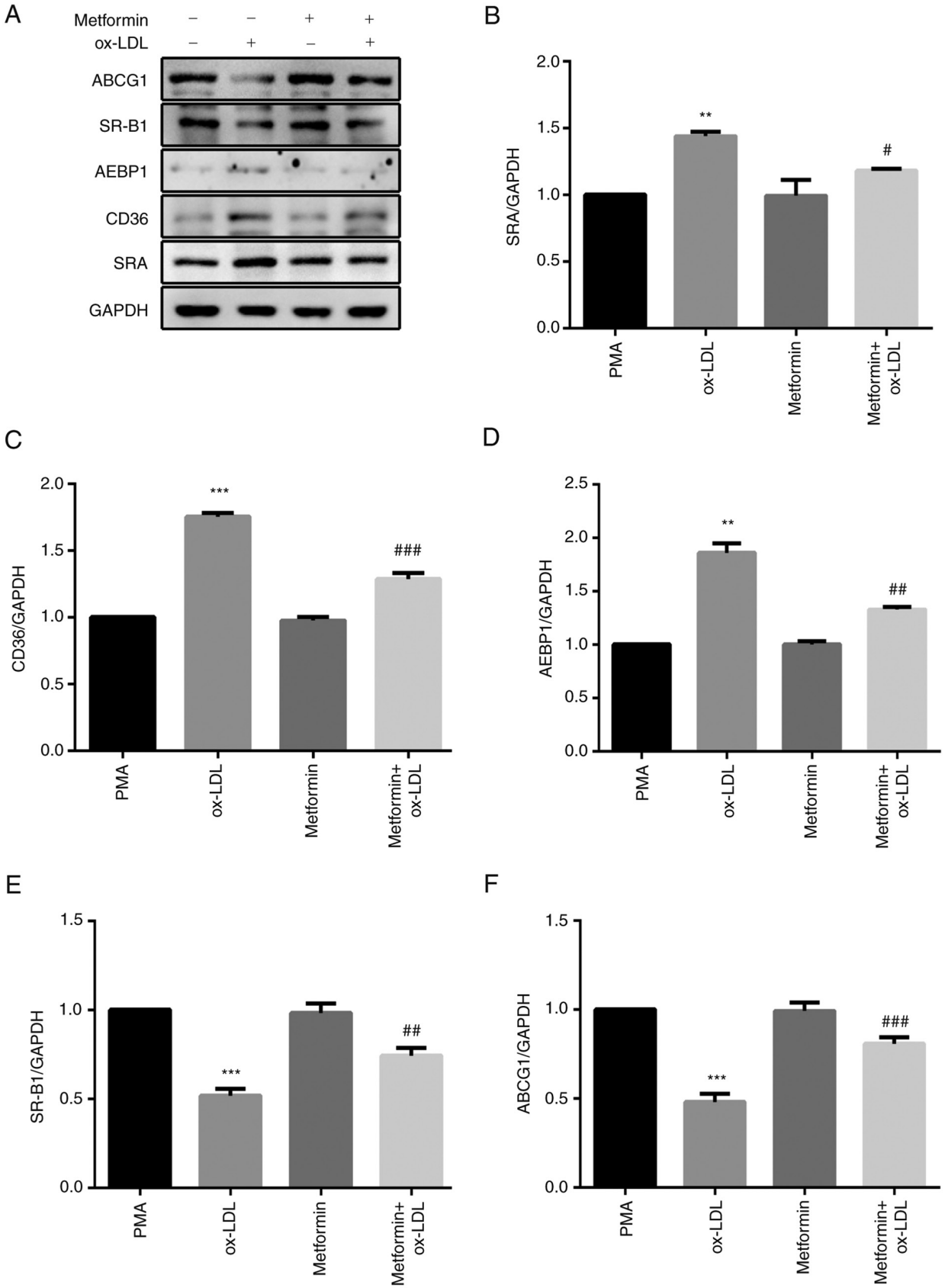

Figure 2. Effects of metformin on SRA, CD36, AEBP1, SR-B1 and ABCG1 expressions in ox-LDL-treated macrophages. (A) Western blot analysis was used to measure the expression levels of SRA, CD36, AEBP1, SR-B1 and ABCG1 proteins following application of the indicated treatments; GAPDH was used as a control for the standardization of the total cellular protein. (B) Quantitative analysis of SRA levels. (C) Quantitative analysis of CD36 levels. (D) Quantitative analysis of AEBP1 levels. (E) Quantitative analysis of SR-B1 levels. (F) Quantitative analysis of ABCG1 levels. The data are expressed as mean ± standard deviation and are representative of three independent experiments. **P<0.01 vs. the PMA group, ***P<0.001 vs. the PMA group, $^{\#}$P<0.05 vs. the ox-LDL group, $^{\#\#}$P<0.01 vs. the ox-LDL group and $^{\#\#\#}$P<0.001 vs. the ox-LDL group. SRA, scavenger receptor A; CD36, cluster of differentiation 36; AEBP1, adipocyte enhancer-binding protein 1; SR-B1, scavenger receptor B1; ABCG1, ATP binding cassette transporter G1; ox-LDL, oxidized low-density lipoprotein; PMA, phorbol 12-myristate 13-acetate.

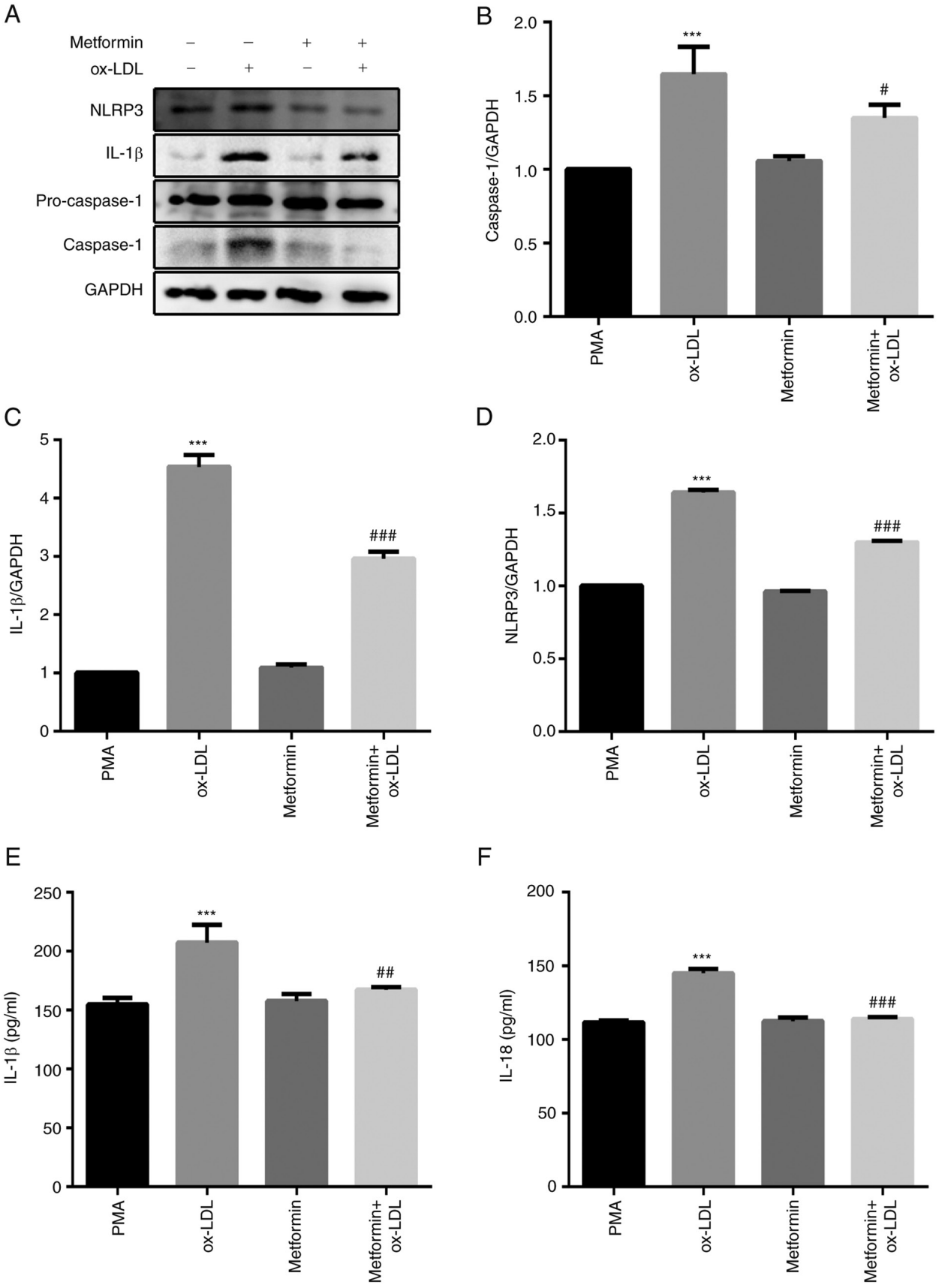

Figure 3. Effects of metformin on the induction of inflammation in ox-LDL-treated macrophages. (A) Western blot analysis indicating the expression levels of caspase-1, IL-1β and NLRP3 following the indicated treatments; GAPDH was used as a control for the standardization of the total cellular protein. (B) Quantitative analysis of caspase-1 levels. (C) Quantitative analysis of IL-1β levels. (D) Quantitative analysis of NLRP3 levels. (E) The expression levels of the cytokine IL-1β were measured in cell culture supernatants by ELISA. (F) The expression levels of the cytokine IL-18 were measured in the cell culture supernatants by ELISA. The data are expressed as mean ± standard deviation and are representative of three independent experiments. ***P<0.001 vs. the PMA group, $^{\#}$P<0.05 vs. the ox-LDL group, $^{\#\#}$P<0.01 vs. the ox-LDL group and $^{\#\#\#}$P<0.001 vs. the ox-LDL group. ox-LDL, oxidized low-density lipoprotein; NLRP3, NOD-like receptor protein 3; PMA, phorbol 12-myristate 13-acetate.

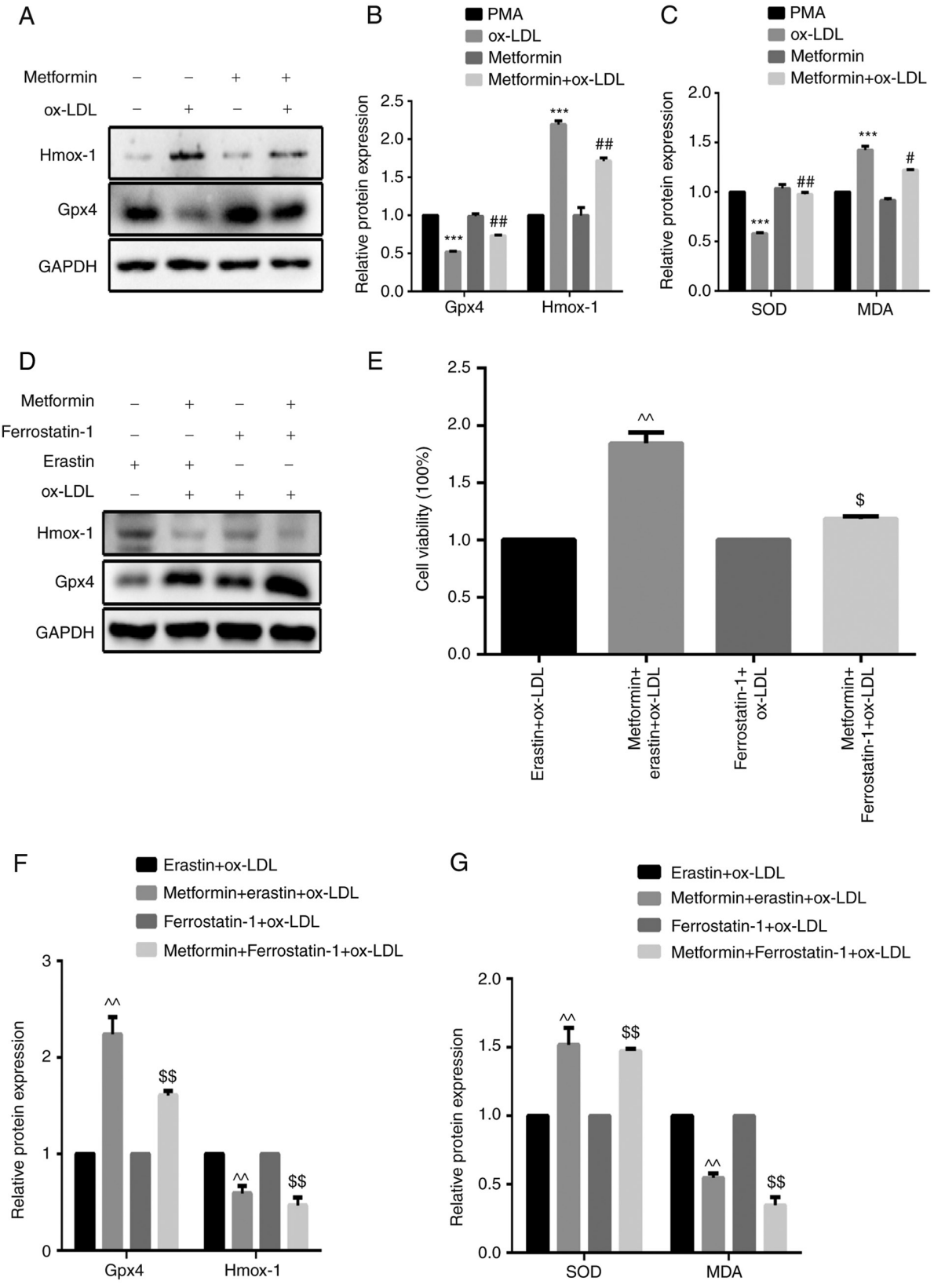

Figure 4. Effects of metformin on the induction of ferroptosis in ox-LDL-treated macrophages. (A) Western blot analysis was used to measure the expression levels of Gpx4 and Hmox-1 proteins following application of the indicated treatments; GAPDH was used as a control for the standardization of the total cellular protein. (B) Quantitative analysis of Gpx4 and Hmox-1 levels. (C) The SOD activity levels in macrophages were detected by the total SOD activity detection kit, The MDA level levels in macrophages were detected by the lipid oxidation (MDA) detection kit. The data are expressed as mean ± standard deviation and were representative of three independent experiments. (D) Western blot analysis was used to measure the expression levels of Gpx4 and Hmox-1 proteins following the indicated treatments; GAPDH was used as a control for the standardization of the total cellular protein. (E) Cell viability was assessed by the CCK-8 assay. (F) Quantitative analysis of GPX4 and Hmox-1 levels. (G) Determination of the SOD and MDA levels in macrophages. ***P<0.001 vs. the PMA group and $^{\#}$P<0.05 vs. the ox-LDL group, $^{\#\#}$P<0.01 vs. the ox-LDL group, $^{\wedge\wedge}$P<0.01 vs. the erastin + ox-LDL group, $^{\$}$P<0.05 vs. the ferrostatin-1 + ox-LDL group, $^{\$\$}$P<0.01 vs. the ferrostatin-1 + ox-LDL group. ox-LDL, oxidized low-density lipoprotein; GPX4, glutathione peroxidase 4; Hmox-1, heme oxygenase-1; SOD, superoxide dismutase; MDA, malondialdehyde; PMA, phorbol 12-myristate 13-acetate.

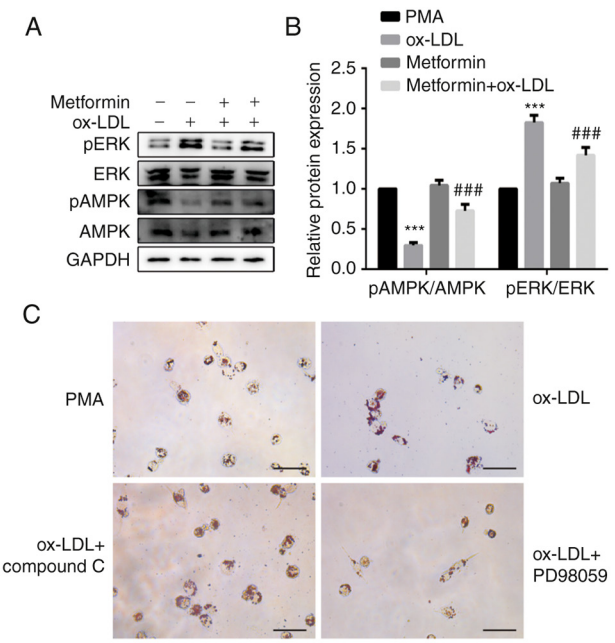

Figure 5. Effects of metformin on the AMPK/ERK signaling pathway in ox-LDL-treated macrophages. (A) Western blot analysis was used to measure the expression levels of AMPK, pAMPK, ERK and pERK proteins following the indicated treatments; GAPDH was used as a control for the standardization of the total cellular protein. (B) Quantitative analysis of the activation of the AMPK and ERK enzymes. (C) Formation of foam cells, as detected by Oil Red O staining. Scale bar=50 μM. ***P<0.001 vs. the PMA group and $^{###}$P<0.001 vs. the ox-LDL group. AMPK, 5' adenosine monophosphate-activated protein kinase; p, phosphorylated; ox-LDL, oxidized low-density lipoprotein; PMA, phorbol 12-myristate 13-acetate.

Discussion

In the present study, metformin inhibited the formation of foam cells in ox-LDL-treated macrophages by decreasing the expression levels of SRA, CD36 and AEBP1 and by increasing the expression levels of SR-B1 and ABCG1. Metformin further suppressed free cholesterol esterification. Pretreatment of the cells with metformin attenuated the inflammatory response in ox-LDL-treated macrophages. In addition, metformin also alleviated the levels of ferroptosis, as demonstrated by the upregulation in the activity levels of Gpx4, the increased activity of SOD, the downregulation noted in the expression levels of Hmox-1 and the decreased concentration levels of MDA. Furthermore, metformin partly reversed the upregulation noted in the levels of ferroptosis caused by erastin and further decreased the downregulation of the levels of ferroptosis in ferrostatin-1-treated macrophages. Moreover, in ox-LDL-stimulated macrophages, metformin induced the activation of AMPK and alleviated the phosphorylation of ERK. The AMPK inhibitor exacerbated these effects, while the ERK inhibitor reversed them.

Foam cell formation is an essential factor in the progression of atherosclerosis (29). The foam cells under the endothelium tend to secrete inflammatory factors to promote local inflammation and the development of an immune response, thereby facilitating the formation of atherosclerotic plaques that contribute to the manifestation of symptoms and inhibit the recovery of patients with atherosclerosis (30). Metformin is a hypoglycemic agent that has been reported to exert a protective role in the development of cardiovascular diseases (31). Previous studies have suggested that metformin inhibits the process of atherosclerosis via the AMPK-PDZ and LIM Domain 5 pathway in diabetic ApoE$^{-/-}$ male mice (26) and reduces the induction of inflammation as demonstrated by the downregulation of the NLRP3 inflammasome (25,32). In the present study, the data indicated that metformin pretreatment inhibited foam cell formation in ox-LDL-treated macrophages. Subsequently, the potential mechanism of this process was examined. The main factor promoting foam cell formation is the accumulation of excessive lipoproteins in monocyte-derived macrophages, which is reflected by cholesterol uptake (SRA, CD36 and AEBP1), cholesterol efflux (SR-B1 and ABCG1) and free cholesterol esterification (33). Therefore, the expression levels of the aforementioned indices and the cholesterol ester/total cholesterol ratio were assessed in the metformin-pretreated ox-LDL-treated macrophage model. The results indicated that metformin inhibited the formation of foam cells by decreasing both the uptake of cholesterol and the esterification of free cholesterol, thereby increasing its efflux in oxLDL-treated THP-1 cells. This result was consistent with the finding reported by a previous study indicating that metformin serves an inhibitory role in cholesterol uptake mediated by sterol regulatory element-binding protein (SREBP) 2 and promotes lipid homeostasis by suppressing oxidative stress induced by AMPK activation (34). Moreover, co-treatment with metformin and the liver X receptor (LXR) agonist T317 increases the expression levels of ABCG1 and ABCA1, reduces monocyte adhesion and proliferation of macrophages, decreases foam cell formation, increases plaque stability and ameliorates progression of atherosclerosis (35). These results suggest that metformin plays a protective effect on foam cell formation in ox-LDL-stimulated macrophages. Consequently, the inhibitory action of metformin on foam cell formation suggested a putative function for this compound as a novel therapeutic agent for atherosclerosis.

In addition, chronic inflammation is a key factor in promoting the process of atherosclerosis (36). A previous study suggests that metformin can reduce macrophage hypoxia inducible factor-1α-dependent proinflammatory signaling (37). The current study explored the specific anti-inflammatory effects of metformin. The data indicated that the expression levels of caspase-1, IL-1β and NLRP3 were decreased and that the secretion of IL-1β and IL-18 was suppressed compared with those noted in the ox-LDL group. This suggested that metformin could reduce the production and secretion of specific inflammatory factors.

The present study indicated that metformin could alleviate the induction of ferroptosis. Moreover, a previous study indicated that iron accumulation in macrophages promoted the formation of foam cells by decreasing the expression levels of ABCA1, ABCG1, LXRα, while it had no effect on the expression of CD36 and lectin-like low-density lipoprotein receptor-1 (38). The present study concluded that iron accumulation ultimately aggravated the development of atherosclerosis. Combined with the results of the current study, it is hypothesized that metformin inhibits lipid accumulation by decreasing induction of ferroptosis in ox-LDL-stimulated macrophages.

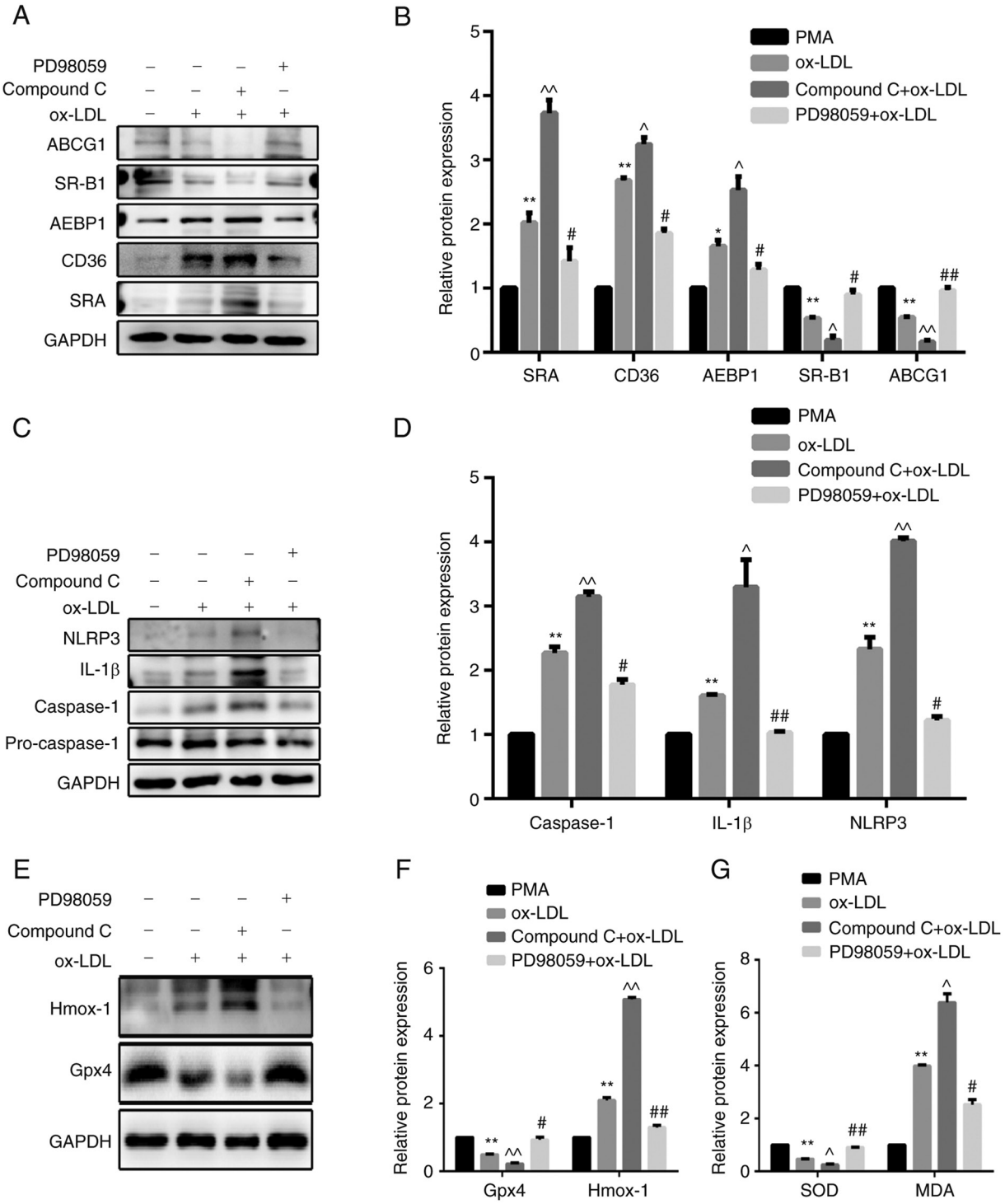

Figure 6. Effects of AMPK/ERK on foam cell formation, inflammation and ferroptosis in ox-LDL-treated macrophages. GAPDH was used as a control for the standardization of the total cellular protein. (A) Western blot analysis was used to measure the expression of cholesterol transport protein following application of the indicated treatments. (B) Quantitative analysis of SRA, CD36, AEBP1, SR-B1 and ABCG1 levels. (C) Western blot analysis was used to measure the expression levels of the inflammatory indices following application of the indicated treatments. (D) Quantitative analysis of caspase-1, IL-1β and NLRP3 levels. (E) Western blot analysis was used to measure the levels of ferroptosis indices following the indicated treatments. (F) Quantitative analysis of Gpx4 and Hmox-1 levels. (G) Determination of the SOD and MDA levels in macrophages. *P<0.05 vs. the PMA group, **P<0.01 vs. the PMA group and $^{\wedge}$P<0.05, $^{\wedge\wedge}$P<0.01 vs. the ox-LDL group, $^{\#}$P<0.05 vs. the ox-LDL group, $^{\#\#}$P<0.01 vs. the ox-LDL group. AMPK, 5' adenosine monophosphate-activated protein kinase; ox-LDL, oxidized low-density lipoprotein; SRA, scavenger receptor A; CD36, cluster of differentiation 36; AEBP1, adipocyte enhancer-binding protein 1; SR-B1, scavenger receptor B1; ABCG1, ATP binding cassette transporter G1; NLRP3, NOD-like receptor protein 3; GPX4, glutathione peroxidase 4; Hmox-1; heme oxygenase-1; PMA, phorbol 12-myristate 13-acetate.

The AMPK signaling pathway is a major intracellular energy metabolism pathway, which serves a protective effect on atherosclerosis by inhibiting inflammation, regulating lipid metabolism, antioxidant activity, as well as suppressing immune responses (39-41). In addition, The ERK/MAPK signaling pathway serves an important role in the process of

atherosclerosis (42). The present study investigated the AMPK and ERK signaling pathways and the data demonstrated that metformin could increase the activation of the AMPK signaling pathway, while decreasing the activation of the ERK pathway in ox-LDL-stimulated THP-1 cells. Moreover, in ox-LDL-treated macrophages, application of an AMPK inhibitor to the cells promoted lipid accumulation, inflammation and increased the levels of ferroptosis, while application of an ERK inhibitor exhibited an opposite effect compared with that noted following treatment of the cells with the AMPK inhibitor.

Studies have shown that metformin moderates the process of atherosclerosis by inhibiting SREBP activity (43), vascular smooth muscle cell migration and autophagy induction (44,45) and it also promotes H2S production, which alleviates atherosclerosis (46). Following pretreatment of the cells with metformin, the data indicated that the AMPK and mammalian target of rapamycin signaling pathways, as well as the Krüppel-like factor 2 protein, a key regulator of the autophagy-lysosome pathway (47) that serves a vital role in regulating the process of atherosclerosis.

In conclusion, the present study provided strong evidence that metformin attenuated the formation of foam cells by downregulating SRA, CD36 and AEBP1 levels and by decreasing free cholesterol esterification, Metformin could also cause an upregulation in the levels of SR-B1 and ABCG1, whereas it alleviated the levels of inflammation and the induction of ferroptosis in ox-LDL-treated THP-1 cells via the AMPK/ERK signaling pathway. These results not only illustrated that metformin can hamper foam cell formation during atherosclerosis but also indicate a potential role for the use of this compound as a therapeutic agent for atherosclerosis.

Acknowledgments

Not applicable.

Funding

The present study was funded by the Health Science and technology plan of Zhejiang Province (grant no. 2021KY203) and the National Natural Science Foundation of China (grant nos. 81671403 and 30871179).

Availability of data and materials

The datasets used and/or analyzed during the current study are available from the corresponding author on reasonable request.

Authors' contributions

YihZ performed the experiments and data analysis and was a major contributor in the writing process of the manuscript. YizZ helped edit the manuscript, and analyzed and interpreted the data. YT and YaZ modified the manuscript and designed the experiments. YihZ and YaZ confirm the authenticity of all the raw data. All authors read and approved the final version of the manuscript.

Ethics approval and consent to participate

Not applicable.

Patient consent for publication

Not applicable.

Competing interests

The authors declare that they have no competing interests.

References

1. Skuratovskaia D, Vulf M, Komar A, Kirienkova E and Litvinova L: Promising directions in atherosclerosis treatment based on epigenetic regulation using MicroRNAs and long noncoding RNAs. Biomolecules 9: 226, 2019.
2. Chistiakov DA, Melnichenko AA, Myasoedova VA, Grechko AV and Orekhov AN: Mechanisms of foam cell formation in atherosclerosis. J Mol Med (Berl) 95: 1153-1165, 2017.
3. Aryal B and Suárez Y: Non-coding RNA regulation of endothelial and macrophage functions during atherosclerosis. Vascul Pharmacol 114: 64-75, 2019.
4. Fang S, Sun S, Cai H, Zou X, Wang S, Hao X, Wan X, Tian J, Li Z, He Z, *et al*: IRGM/Irgm1 facilitates macrophage apoptosis through ROS generation and MAPK signal transduction: $Irgm1^{+/-}$ mice display increases atherosclerotic plaque stability. Theranostics 11: 9358-9375, 2021.
5. Liu S, Sui Q, Zhao Y and Chang X: Lonicera caerulea berry polyphenols activate SIRT1, enhancing inhibition of Raw264.7 macrophage foam cell formation and promoting cholesterol efflux. J Agric Food Chem 67: 7157-7166, 2019.
6. Mofidi R, Crotty TB, McCarthy P, Sheehan SJ, Mehigan D and Keaveny TV: Association between plaque instability, angiogenesis and symptomatic carotid occlusive disease. Br J Surg 88: 945-950, 2001.
7. Falk E: Pathogenesis of atherosclerosis. J Am Coll Cardiol 47 (8 Suppl): C7-C12, 2006.
8. Wang Y, Zhao Y, Wang H, Zhang C, Wang M, Yang Y, Xu X and Hu Z: Histone demethylase KDM3B protects against ferroptosis by upregulating SLC7A11. FEBS Open Bio 10: 637-643, 2020.
9. Latunde-Dada GO: Ferroptosis: Role of lipid peroxidation, iron and ferritinophagy. Biochim Biophys Acta Gen Subj 1861: 1893-1900, 2017.
10. Stockwell BR, Friedmann Angeli JP, Bayir H, Bush AI, Conrad M, Dixon SJ, Fulda S, Gascón S, Hatzios SK, Kagan VE, *et al*: Ferroptosis: A regulated cell death nexus linking metabolism, redox biology, and disease. Cell 171: 273-285, 2017.
11. Bai T, Li M, Liu Y, Qiao Z and Wang Z: Inhibition of ferroptosis alleviates atherosclerosis through attenuating lipid peroxidation and endothelial dysfunction in mouse aortic endothelial cell. Free Radic Biol Med 160: 92-102, 2020.
12. Zhou Y, Zhou H, Hua L, Hou C, Jia Q, Chen J, Zhang S, Wang Y, He S and Jia E: Verification of ferroptosis and pyroptosis and identification of PTGS2 as the hub gene in human coronary artery atherosclerosis. Free Radic Biol Med 171: 55-68, 2021.
13. Sindrilaru A, Peters T, Wieschalka S, Baican C, Baican A, Peter H, Hainzl A, Schatz S, Qi Y, Schlecht A, *et al*: An unrestrained proinflammatory M1 macrophage population induced by iron impairs wound healing in humans and mice. J Clin Invest 121: 985-997, 2011.
14. Martinet W, Coornaert I, Puylaert P and De Meyer GRY: Macrophage death as a pharmacological target in atherosclerosis. Front Pharmacol 10: 306, 2019.
15. Flory J and Lipska K: Metformin in 2019. JAMA 321: 1926-1927, 2019.
16. Anselmino LE, Baglioni MV, Malizia F, Laluce NC, Etichetti CB, Marignac VLM, Rozados V, Scharovsky OG, Girardini J, Rico MJ and Menacho Márquez M: Repositioning metformin and propranolol for colorectal and triple negative breast cancers treatment. Sci Rep 11: 8091, 2021.
17. Chen J, Zhou C, Yi J, Sun J, Xie B, Zhang Z, Wang Q, Chen G, Jin S, Hou J, *et al*: Metformin and arsenic trioxide synergize to trigger Parkin/pink1-dependent mitophagic cell death in human cervical cancer HeLa cells. J Cancer 12: 6310-6319, 2021.
18. Chen YH, Wu JX, Yang SF, Chen ML, Chen TH and Hsiao YH: Metformin potentiates the anticancer effect of everolimus on cervical cancer in vitro and in vivo. Cancers (Basel) 13: 4612, 2021.

19. Klose K, Packeiser EM, Muller P, Granados-Soler JL, Schille JT, Goericke-Pesch S, Kietzmann M, Murua Escobar H aand Nolte I: Metformin and sodium dichloroacetate effects on proliferation, apoptosis, and metabolic activity tested alone and in combination in a canine prostate and a bladder cancer cell line. PLoS One 16: e0257403, 2021.
20. Tseng HH, Chen YZ, Chou NH, Chen YC, Wu CC, Liu LF, Yang YF, Yeh CY, Kung ML, Tu YT and Tsai KW: Metformin inhibits gastric cancer cell proliferation by regulation of a novel Loc100506691-CHAC1 axis. Mol Ther Oncolytics 22: 180-194, 2021.
21. Xiong W, Sun KY, Zhu Y, Zhang X, Zhou YH and Zou X: Metformin alleviates inflammation through suppressing FASN-dependent palmitoylation of Akt. Cell Death Dis 12: 934, 2021.
22. Raffort J, Hassen-Khodja R, Jean-Baptiste E and Lareyre F: Relationship between metformin and abdominal aortic aneurysm. J Vasc Surg 71: 1056-1062, 2020.
23. Du F, Cao Y, Ran Y, Wu Q and Chen B: Metformin attenuates angiotensin II-induced cardiomyocyte hypertrophy by upregulating the MuRF1 and MAFbx pathway. Exp Ther Med 22: 1231, 2021.
24. Loi H, Kramar S, Laborde C, Marsal D, Pizzinat N, Cussac D, Roncalli J, Boal F, Tronchere H, Oleshchuk O, *et al*: Metformin attenuates postinfarction myocardial fibrosis and inflammation in mice. Int J Mol Sci 22: 9393, 2021.
25. Vasamsetti SB, Karnewar S, Kanugula AK, Thatipalli AR, Kumar JM and Kotamraju S: Metformin inhibits monocyte-to-macrophage differentiation via AMPK-mediated inhibition of STAT3 activation: Potential role in atherosclerosis. Diabetes 64: 2028-2041, 2015.
26. Tang G, Duan F, Li W, Wang Y, Zeng C, Hu J, Li H, Zhang X, Chen Y and Tan H: Metformin inhibited Nod-like receptor protein 3 inflammasomes activation and suppressed diabetes-accelerated atherosclerosis in apoE$^{-/-}$ mice. Biomed Pharmacother 119: 109410, 2019.
27. Yan Y, Li T, Li Z, He M, Wang D, Xu Y, Yang X, Bai Y, Lao Y, Zhang Z and Wu W: Metformin suppresses the progress of diabetes-accelerated atherosclerosis by inhibition of vascular smooth muscle cell migration through AMPK-Pdlim5 pathway. Front Cardiovasc Med 8: 690627, 2021.
28. Tsuchiya S, Kobayashi Y, Goto Y, Okumura H, Nakae S, Konno T and Tada K: Induction of maturation in cultured human monocytic leukemia cells by a phorbol diester. Cancer Res 42: 1530-1536, 1982.
29. Lightbody RJ, Taylor JMW, Dempsie Y and Graham A: MicroRNA sequences modulating inflammation and lipid accumulation in macrophage 'foam' cells: Implications for atherosclerosis. World J Cardiol 12: 303-333, 2020.
30. Leong XF: Lipid oxidation products on inflammation-mediated hypertension and atherosclerosis: A mini review. Front Nutr 8: 717740, 2021.
31. Larsen AH, Jessen N, Norrelund H, Tolbod LP, Harms HJ, Feddersen S, Nielsen F, Brøsen K, Hansson NH, Frøkiaer J, *et al*: A randomised, double-blind, placebo-controlled trial of metformin on myocardial efficiency in insulin-resistant chronic heart failure patients without diabetes. Eur J Heart Fail 22: 1628-1637, 2020.
32. Xu W, Deng YY, Yang L, Zhao S, Liu J, Zhao Z, Wang L, Maharjan P, Gao S, Tian Y, *et al*: Metformin ameliorates the proinflammatory state in patients with carotid artery atherosclerosis through sirtuin 1 induction. Transl Res 166: 451-458, 2015.
33. Wang D, Yang Y, Lei Y, Tzvetkov NT, Liu X, Yeung AWK, Xu S and Atanasov AG: Targeting foam cell formation in atherosclerosis: Therapeutic potential of natural products. Pharmacol Rev 71: 596-670, 2019.
34. Gopoju R, Panangipalli S and Kotamraju S: Metformin treatment prevents SREBP2-mediated cholesterol uptake and improves lipid homeostasis during oxidative stress-induced atherosclerosis. Free Radic Biol Med 118: 85-97, 2018.
35. Ma C, Zhang W, Yang X, Liu Y, Liu L, Feng K, Zhang X, Yang S, Sun L, Yu M, *et al*: Functional interplay between liver X receptor and AMP-activated protein kinase α inhibits atherosclerosis in apolipoprotein E-deficient mice-a new anti-atherogenic strategy. Br J Pharmacol 175: 1486-1503, 2018.
36. Greaves DR and Gordon S: Thematic review series: The immune system and atherogenesis. Recent insights into the biology of macrophage scavenger receptors. J Lipid Res 46: 11-20, 2005.
37. Pescador N, Francisco V, Vázquez P, Esquinas EM, González-Páramos C, Valdecantos MP, García-Martínez I, Urrutia AA, Ruiz L, Escalona-Garrido C, *et al*: Metformin reduces macrophage HIF1α-dependent proinflammatory signaling to restore brown adipocyte function in vitro. Redox Biol 48: 102171, 2021.
38. Cai J, Zhang M, Liu Y, Li H, Shang L, Xu T, Chen Z, Wang F, Qiao T and Li K: Iron accumulation in macrophages promotes the formation of foam cells and development of atherosclerosis. Cell Biosci 10: 137, 2020.
39. Hu R, Wang MQ, Ni SH, Wang M, Liu LY, You HY, Wu XH, Wang YJ, Lu L and Wei LB: Salidroside ameliorates endothelial inflammation and oxidative stress by regulating the AMPK/NF-κB/NLRP3 signaling pathway in AGEs-induced HUVECs. Eur J Pharmacol 867: 172797, 2020.
40. Fullerton MD, Steinberg GR and Schertzer JD: Immunometabolism of AMPK in insulin resistance and atherosclerosis. Mol Cell Endocrinol 366: 224-234, 2013.
41. Yong Z, Ruiqi W, Hongji Y, Ning M, Chenzuo J, Yu Z, Zhixuan X, Qiang L, Qibing L, Weiying L and Xiaopo Z: Mangiferin ameliorates HFD-Induced NAFLD through regulation of the AMPK and NLRP3 inflammasome signal pathways. J Immunol Res 2021: 4084566, 2021.
42. Ding J, Li Z, Li L, Ding Y, Wang D, Meng S, Zhou Q, Gui S, Wei W, Zhu H and Wang Y: Myosin light chain kinase inhibitor ML7 improves vascular endothelial dysfunction and permeability via the mitogen-activated protein kinase pathway in a rabbit model of atherosclerosis. Biomed Pharmacother 128: 110258, 2020.
43. Li Y, Xu S, Mihaylova MM, Zheng B, Hou X, Jiang B, Park O, Luo Z, Lefai E, Shyy JY, *et al*: AMPK phosphorylates and inhibits SREBP activity to attenuate hepatic steatosis and atherosclerosis in diet-induced insulin-resistant mice. Cell Metab 13: 376-388, 2011.
44. Wu H, Feng K, Zhang C, Zhang H, Zhang J, Hua Y, Dong Z, Zhu Y, Yang S and Ma C: Metformin attenuates atherosclerosis and plaque vulnerability by upregulating KLF2-mediated autophagy in apoE$^{-/-}$ mice. Biochem Biophys Res Commun 557: 334-341, 2021
45. Li S, Shi Y, Liu P, Song Y, Liu Y, Ying L, Quan K, Yu G, Fan Z and Zhu W: Metformin inhibits intracranial aneurysm formation and progression by regulating vascular smooth muscle cell phenotype switching via the AMPK/ACC pathway. J Neuroinflammation 17: 191, 2020.
46. Ma X, Jiang Z, Wang Z and Zhang Z: Administration of metformin alleviates atherosclerosis by promoting H2S production via regulating CSE expression. J Cell Physiol 235: 2102-2112, 2020.
47. You G, Long X, Song F, Huang J, Tian M, Xiao Y, Deng S and Wu Q: Metformin activates the AMPK-mTOR pathway by modulating lncRNA TUG1 to induce autophagy and inhibit atherosclerosis. Drug Des Devel Ther 14: 457-468, 2020.